0013-7227/01/$03.00/0
Printed in U.S.A.

Endocrinology 142(11):5005–5014

Gonadal Pathologies in Transgenic Mice Expressing the Rat Inhibin α-Subunit

MICHELLE L. McMULLEN, BYUNG-NAM CHO*, C. JEANA YATES, AND KELLY E. MAYO

Department of Biochemistry, Molecular Biology, and Cell Biology, and Center for Reproductive Science, Northwestern University, Evanston, Illinois 60208

Inhibin and activin are structurally related dimeric peptide hormones and are members of the TGF-β superfamily of proteins. In the accompanying paper, we describe transgenic mice that overexpress the inhibin α-subunit gene from a metallothionein-I promoter (MT-α) and examine the effects of the MT-α transgene on gonadotropin levels and fertility. To characterize the effects of increased inhibin α-subunit on gonadal morphology and function, in this report we investigate gonadal histology, steroid hormone levels, and the basis of ovarian cyst formation in MT-α transgenic mice. MT-α transgenic female mice develop large fluid-filled ovarian cysts of follicular origin as early as 3 months of age. By 12 months of age, more than 92% of female MT-α transgenic mice develop ovarian cysts compared with less than 25% of wild-type littermates. Ovarian cysts form unilaterally or bilaterally, and cystic ovaries often have a greatly expanded bursal sac. Additionally, the ovaries of MT-α transgenic mice contain polyovular follicles and have fewer mature antral follicles and corpora lutea. MT-α female mice exhibit abnormal steroid hormone production, with increased serum T levels and reductions in serum E with corresponding reductions in uterine mass. In the MT-α transgenic males, testis size was decreased by 20–40% compared with control males, and there is a corresponding reduction in seminiferous tubule volume. After a chronic treatment with a GnRH antagonist, MT-α female mice continued to develop ovarian cysts and bursal sac expansions, although the cysts were markedly reduced in size. These results indicate that the expression of the rat inhibin α-subunit in mice results in significant ovarian pathology, reduced testicular size, and altered ovarian steroidogenesis. The antagonist studies are consistent with a direct ovarian effect of the α-subunit transgene product mediated by changes in the inhibin-to-activin ratio in these mice. (*Endocrinology* 142: 5005–5014, 2001)

THE INHIBINS AND activins were isolated as gonadal proteins that stimulate, or inhibit, respectively, FSH synthesis and secretion (1–6). In addition to their endocrine role, inhibin and activin are also likely to function as intragonadal autocrine and paracrine factors (7, 8). Treatment of ovarian cells with either inhibin or activin results in cell-specific alterations of ovarian functions, such as changes in basal and gonadotropin-induced steroid and cAMP production (9). Activin stimulates basal and FSH-induced production of inhibin protein and α- and β_A-subunit mRNA expression (10). Additionally, activins and inhibins affect ovarian follicular growth, development, atresia, and steroidogenesis as well as testicular spermatogonial production (8, 11, 12). Injection of inhibin into the rat ovarian bursa causes an increase in the size and number of follicles and increased thymidine incorporation into DNA (7). Activin acts in an opposite manner to decrease granulosa cell proliferation and increase atresia of antral follicles (7). Inhibin stimulates LH-induced androgen production in rat theca cells and Leydig cells, an effect that is blocked by activin (11). In the testis, inhibin decreases spermatogonial proliferation when injected locally. Conversely, activin stimulates spermatogonial proliferation (8). These data suggest that inhibin and activin can function as autocrine/paracrine factors within the gonad and are often functional antagonists.

The potential role of inhibin in the pathogenesis of ovarian disease is unclear. Increased inhibin activity has been associated with polycystic ovarian disease in some studies (13–15) and with juvenile granulosa cell tumors (16, 17). Inhibin A has also been suggested to be a useful marker for mucinous epithelial cell tumors in women (16) and a prognostic factor for the survival of postmenopausal women with epithelial ovarian carcinoma (18). Granulosa-theca cell tumors in mares are also known to express high levels of inhibin (19). Mice that are deficient for the inhibin α-subunit gene develop gonadal stromal tumors, adrenal cortical tumors, a cachexia-like wasting syndrome, and are infertile (20, 21). These observations indicate that increased inhibin levels or conversely lack of inhibin is often associated with ovarian pathogenesis. This suggests that inhibin may exert direct autocrine/paracrine effects within the ovary.

Although abnormal inhibin levels have been associated with ovarian pathology, it has been difficult to establish a cause-and-effect relationship between inhibin and ovarian disorders. To establish the importance of inhibin and the related hormone activin in gonadal function and in reproductive disorders, transgenic mice have been generated that overexpress the inhibin α-subunit gene. These animals provide a useful *in vivo* system for examining the actions of inhibin and activin within the intact animal. Metallothionein-I promoter (MT-α) transgenic mice exhibit abnormal gonadotropin levels and female subfertility, as described in the accompanying paper. This report focuses on the effect of inhibin α-subunit overexpression on gonadal steroidogenesis and morphology and describes the resulting ovarian pathologies.

Abbreviations: ERKO, E receptor-deficient mice; hCG, human CG; MT-α, metallothionein-I promoter inhibin α-subunit; PCOS, polycystic ovarian syndrome.

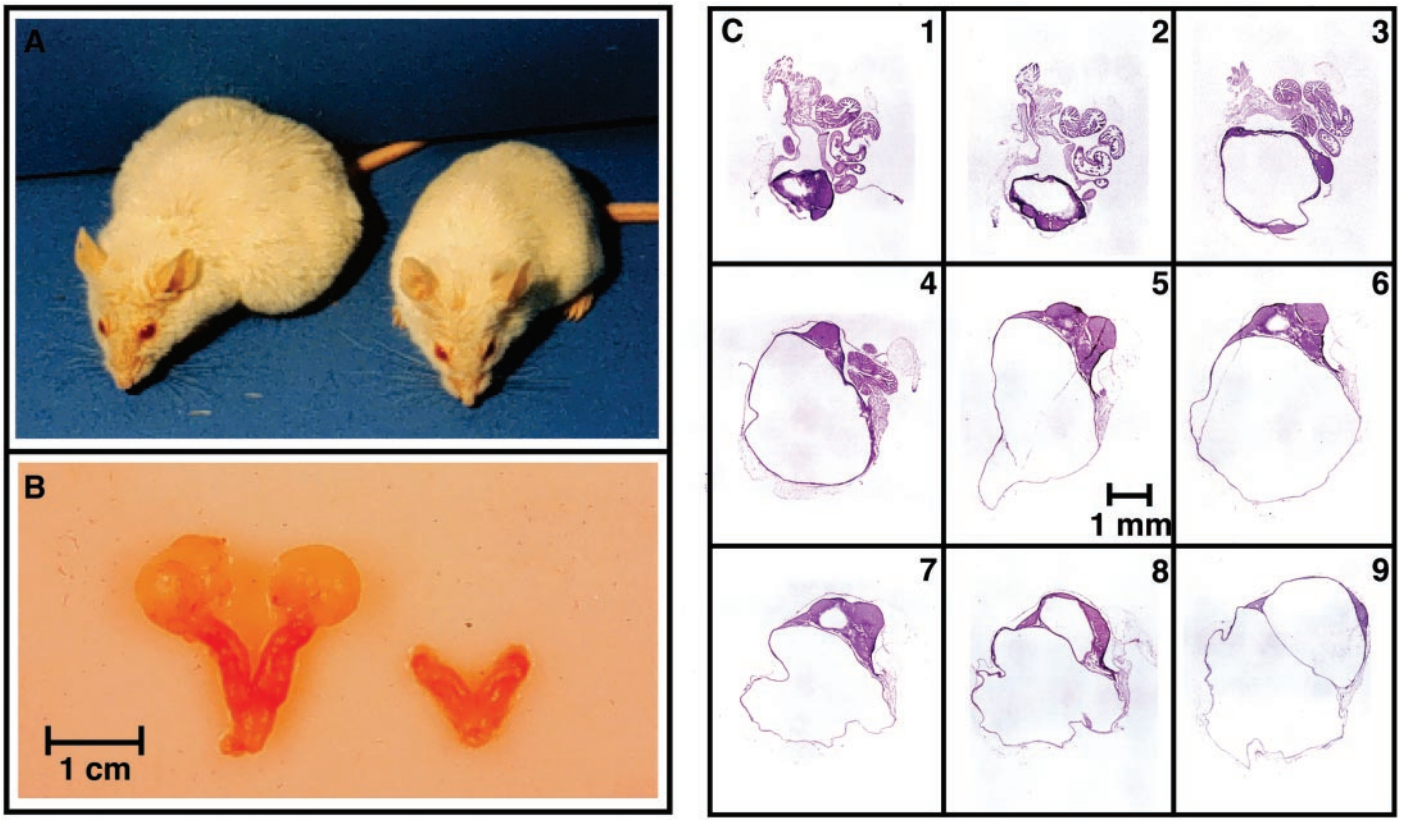

FIG. 1. Characteristics of a line of transgenic mice that overexpress the inhibin α-subunit gene. A, A 1-yr-old line C transgenic female mouse (*left*) and a control littermate (*right*). Note the distended abdomen of the transgenic animal. B, The ovaries and uterus of a 1-year-old line C MT-α transgenic female mouse (*left*) and a control littermate (*right*). The bursal sacs of both transgenic ovaries are filled with clear fluid. C, Panels 1–9 represent 20-μm sequential sections through a MT-α transgenic ovary. Two very large follicular cysts are apparent, one beginning in panel 1 and the other beginning in panel 6. In addition, the bursal sac of this ovary was filled with fluid before fixation.

Materials and Methods

Generation and maintenance of transgenic mice

The generation of MT-α transgenic mice is described in detail in the accompanying paper. A 1.4-kb rat inhibin α cDNA was cloned into the vector pEV142 (provided by Dr. Richard Palmiter, University of Washington, Seattle), which includes a mouse MT-α and a human GH RNA processing and polyadenylation site (22, 23). Transgenic animals were produced at the Northwestern University-Markey Developmental Biology Center Core Facility under the direction of Dr. Phillip Iannoccone. Genomic DNA was isolated from tail biopsies of the 11 F_0 mice born. Three founder male mice were identified using the 1.4-kb rat inhibin α cDNA as a hybridization probe. The males were used to establish three separate transgenic lines, lines A–C. All subsequent generations were raised in a room with a controlled photoperiod (14 h of light, 10 h of dark) and temperature (22–25 C). All lines stably transmit the transgene at the expected 50% Mendelian frequency.

Ovarian cyst analysis and gonadal histology

Ovaries of MT-α transgenic and wild-type mice were examined for the gross appearance of ovarian cysts. Animals were distributed into three groups according to age: 3–7 months, 8–12 months, and older than 12 months. Cysts were categorized based on size as small (<5 mm diameter) and large (>5 mm diameter). Testes were removed and weighed before fixation. The excised ovaries and testes were immediately fixed in fresh 4% paraformaldehyde in PBS, pH 7.4. After overnight fixation, tissues were dehydrated in ethanol and embedded in paraffin. Sections of ovaries and testes (4–6 μm) were prepared using a Reichert-Jung microtome (Cambridge Instruments, Inc., Buffalo, NY). Ovaries with large cysts were sectioned at 10–20 μm to maintain tissue integrity. The sections were deparaffinized with xylene, dehydrated in absolute ethanol, and rehydrated in water. Sections were stained with eosin and counterstained with hematoxylin. Ovaries examined in the polyovular follicle study were prepared as described above and then completely sectioned at 6 μm. All sections were examined at ×100 and ×400 and/or ×1000 magnification. Polyovular follicles spanned several serial sections; however, only distinctly different polyovular follicles were counted.

Hormone measurements

All female mice were cycled before collection of serum for hormone analysis. Estrous cycle stages were determined by daily examination of vaginal cytology. Those animals demonstrating a minimum of two consecutive 4- to 5-d cycles were killed on the morning of metestrus or diestrus. Ovarian cyst fluid was collected with a 26.5-gauge needle and syringe and stored at −80 C until the inhibin α-chain RIA was performed. Serum and cyst fluid hormone measurements were determined by RIA at the Northwestern University P30 Center RIA Core Facility under the direction of Drs. John Levine and Neena Schwartz. National Institute of Diabetes and Digestive and Kidney Diseases antiserum and standards (rLH-RP-3 standard/rLH-S-11 antibody and rFSH-RP-2 standard/rFSH-S-11 antibody) were used for LH and FSH measurements. FSH and LH results are expressed as nanograms per milliliter. FSH assay sensitivity was 0.05 ng/sample or 1.0 ng/ml, and LH assay sensitivity was 0.01 ng/sample or 0.2 ng/ml. A T double antibody RIA kit (ICN, Costa Mesa, CA) and E double antibody RIA kit (Diagnostic Products Corp., Los Angeles, CA) containing antibodies and standards were used for T and E RIAs. Both T assay and E assay sensitivity was at 2.0 pg/ml. Animals used in the steroid studies ranged from 6 to 12 months of age. Reagents (Tyr 27 rat inhibin α 1–27 standard/sheep anti-Tyr 27 rat inhibin α 1–27 antibody 795) provided by Dr. Wylie Vale (Salk Institute, San Diego, CA) were used for the inhibin α-chain assay as described (24,

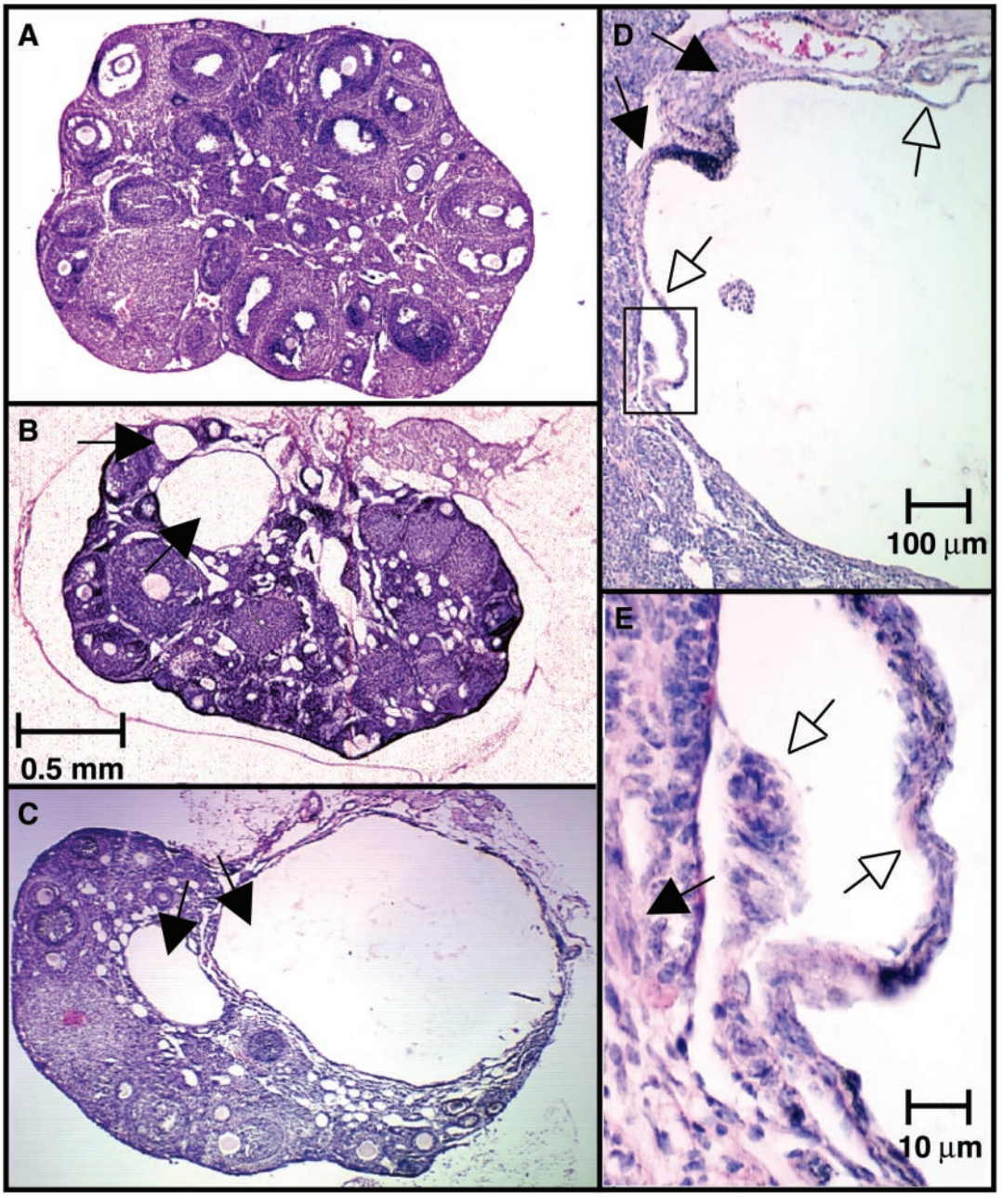

FIG. 2. Ovarian histology of MT-α transgenic mice. Ovaries were fixed in 4% paraformaldehyde in PBS, embedded in paraffin, sectioned, and stained with hematoxylin and eosin ($\times$28 magnification). A, A 5-μm section of an ovary from a 9-month-old wild-type littermate. B, A 20-μm section of an ovary from a 9-month-old line C MT-α female. C, A 20-μm section of an ovary from a 9-month-old line A MT-α female. Multiple cysts, which are present in both ovaries, are designated by *arrows* in B and C. D, Magnification ($\times$100) of a different serial section from the same MT-α ovary shown in C. E, Magnification ($\times$1000) of the edge of the cyst shown in D. *Open arrows* point to cells with granulosa cell morphology and *closed arrows* point to cells with thecal cell morphology in D and E.

25). Results are expressed as picomoles per milliliter. The interassay coefficients of variation were 12.0%, 12.0%, and 9.3% for T, E, and inhibin, respectively.

GnRH antagonist treatment

Six-week-old MT-α transgenic and wild-type littermate female mice were used in this study. The GnRH antagonist Cetrorelix (Asta Medica, Frankfurt, Germany) was administered by injection at a dosage of 10 mg/kg body weight every 84 h for 4.5 months to 5 MT-α C-line females, 5 MT-α A-line females, and 10 wild-type females. A vehicle (water) injection of the same volume was administered to 4 MT-α C-line females, 5 MT-α A-line females, and 10 wild-type females as a control. Animals were killed 2–3 days after the last injection. Serum samples were collected, gross ovarian morphology was examined, and ovaries were fixed in 4% paraformaldehyde and embedded in paraffin as described above for subsequent histological analysis.

Results

Ovarian pathology

To determine the effects of inhibin α-subunit transgene expression on ovarian morphology, both gross and micro-

scopic histological analyses of ovaries from MT-α transgenic mice were performed. The most striking ovarian phenotype for the MT-α transgenic females was the development of large fluid-filled ovarian cysts (Fig. 1). The cysts can be large enough to distend the abdomen of MT-α female mice (Fig. 1A). The bursal sac of cystic ovaries is often expanded and filled with clear fluid (Fig. 1B). Serial sectioning of MT-α ovaries revealed that multiple cysts are usually present within a single ovary, with an observed range of one to three cysts per ovary (Fig. 1C).

Microscopic examination of MT-α ovaries revealed additional smaller ovarian cysts not apparent by gross examination (Fig. 2, A–C). Also, transgenic ovaries are slightly smaller than control ovaries, and in general they exhibit fewer tertiary follicles, antral follicles, and corpora lutea. The periphery of the MT-α ovarian cysts are lined with several thin discontinuous layers of cuboidal cells that appear to be remnants of the granulosa cell layer cells (Fig. 2, D–E, open arrows). *In situ* hybridization analysis as described in the accompanying paper revealed no expression of the inhibin α-subunit or LH receptor mRNA in these cells (not shown),

TABLE 1. Percentage of mice that developed ovarian cysts

	Wild type	MT-α line A	MT-α line C
3–7 months	19 (n = 37)	50 (n = 18)	79 (n = 14)
8–12 months	26 (n = 27)	58 (n = 19)	91 (n = 11)
Older than 12 months	25 (n = 8)	92 (n = 13)	92 (n = 13)
Total	22 (n = 72)	64 (n = 50)	87 (n = 38)

The rate of cyst formation is significantly different between transgenic lines and wild-type controls. The rate of cyst formation is significantly different between the age groups of MT-α line A, MT-α line C, and wild-type controls. Statistical analyses were performed using χ^2 goodness of fit based on 2 degrees of freedom and χ^2 sums greater than a 0.95 *P* level.

TABLE 2. Percentage of mice with large cysts *vs.* small cysts

	Wild type (n = 72)	MT-α line A (n = 50)	MT-α line C (n = 38)
Large (>5 mm)	12	38	66
Small (<5 mm)	10	26	21
No cyst	78	36	13

The percentages represent female mice exhibiting unilateral or bilateral ovarian cysts. A significant difference in the frequency of large cysts and the frequency of no cysts exists between transgenic lines and wild-type controls. Statistical analyses were performed using χ^2 goodness of fit based on 2 degrees of freedom and χ^2 sums greater than a 0.95 *P* level.

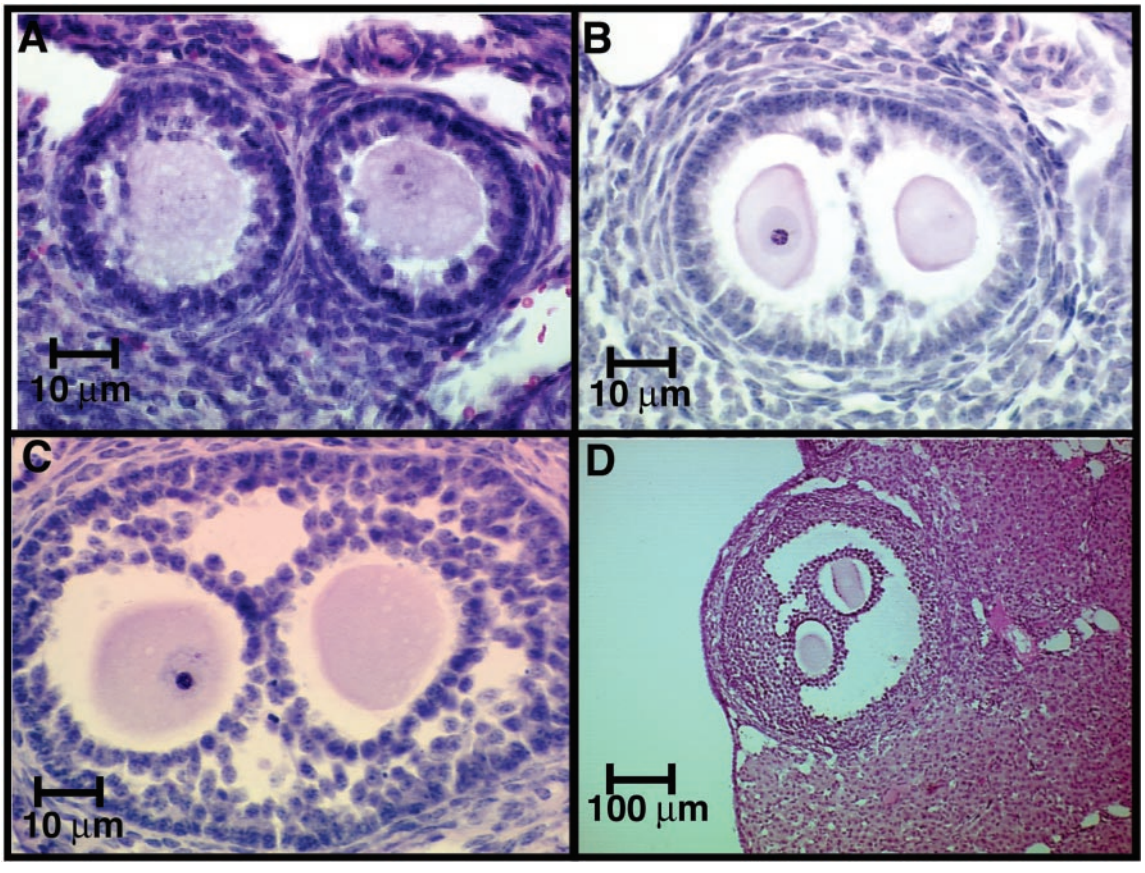

FIG. 3. Follicular histology of polyovular follicles from MT-α transgenic ovaries. Ovaries from MT-α transgenic mice (n = 11) and wild-type mice (n = 10) were fixed in 4% paraformaldehyde in PBS and embedded in paraffin. One ovary from each animal was completely sectioned at 4–6 μm and stained with hematoxylin and eosin. A, Normal adjacent primary follicles from a wild-type ovary; B, MT-α transgenic preantral polyovular follicle; C, MT-α transgenic early antral polyovular follicle; D, MT-α transgenic late antral polyovular follicle. Magnification, ×100 in A and ×1000 in B–D.

so they do not appear to be healthy granulosa cells. The MT-α cystic follicles have an additional outer layer of flat, striated cells that exhibit the fibroblast-like morphology of a theca layer (Fig. 2, D–E, solid arrows). Cyst aspirates collected from both MT-α and wild-type ovaries were measured for inhibin α levels by RIA. The total inhibin levels present in MT-α transgenic cyst fluid were 6-fold greater (4.31 $\pm$ 1.07 pmol/ml) than fluid collected from wild-type mice with ovarian cysts (0.71 $\pm$ 0.31 pmol/ml) ($P < 0.05$). Serum total inhibin levels were increased in MT-α transgenic animals by approximately 2-fold, as described in the accompanying paper (25a).

The overall rate of cyst formation in transgenic mice was 64% for line A and 87% for line C (Table 1). The incidence of ovarian cysts varies between mouse strains and with age (26). Therefore, to establish the basal rate of cyst formation in the background strain of MT-α transgenic mice, CD-1, we examined ovaries from nontransgenic littermates at a range of ages. The average rate of cyst formation for all ages of nontransgenic littermates was 22%. The frequency of cyst formation in MT-α transgenic females increases with age. Fifty to 79% of MT-α females from 3–7 months of age develop ovarian cysts, 58–91% of MT-α females from 8–12 months of age develop ovarian cysts, and more than 90% of MT-α females older than 1 yr develop ovarian cysts (Table 1). Cysts from wild-type ovaries are typically very small (<5 mm), and these mice generally have only one cyst per ovary. Cysts from transgenic females are much larger (>5 mm) (Table 2), and these animals typically display two or more cysts per ovary. The incidence of large ovarian cysts is statistically greater in transgenic females compared with wild-type littermates.

In addition to the cyst pathology, transgenic ovaries also exhibit polyovular follicles (Fig. 3). The majority of the follicles with two ova are late preantral or early antral follicles (Fig. 3, B and C), but a few large late antral follicles were also observed (Fig. 3A). A group of transgenic and control ovaries were completely sectioned at 4–6 μm. Subsequently, each section was examined for the presence of polyovular follicles (27). On average, MT-α transgenic ovaries contained three polyovular follicles per ovary (line A, 2.8 $\pm$ 0.4, n = 6; line C, 3.0 $\pm$ 0.0, n = 5). Of the 10 wild-type ovaries examined, only one polyovular follicle was observed (0.1 $\pm$ 0.1, n = 10).

Testicular pathology

In contrast to MT-α transgenic females, MT-α transgenic males are fertile, despite reduced sperm production. We have observed that in MT-α male transgenic mice, testis size is decreased (line A, 125.5 $\pm$ 16.7 mg per pair of testes, n = 4; line C, 168.3 $\pm$ 8.1 mg per pair of testes, n = 7) compared with nontransgenic male littermates (208.8 $\pm$ 12.7 mg per pair of testes, n = 10, $P < 0.01$) (Fig. 4, A and B). This reduction in testis size is associated with reduced seminiferous tubule volume (Fig. 4, C and D). Seminiferous tubule diameters were significantly reduced in transgenic male mice (line A, 82.8 $\pm$ 1 5.3 μm; line C, 112.3 $\pm$ 2.4 μm; wild-type, 157.0 $\pm$ 5.3 μm; $P < 0.0001$). Histological studies revealed fewer mature sperm within most seminiferous tubules of MT-α males, consistent with reduced sperm counts shown in the accompanying paper.

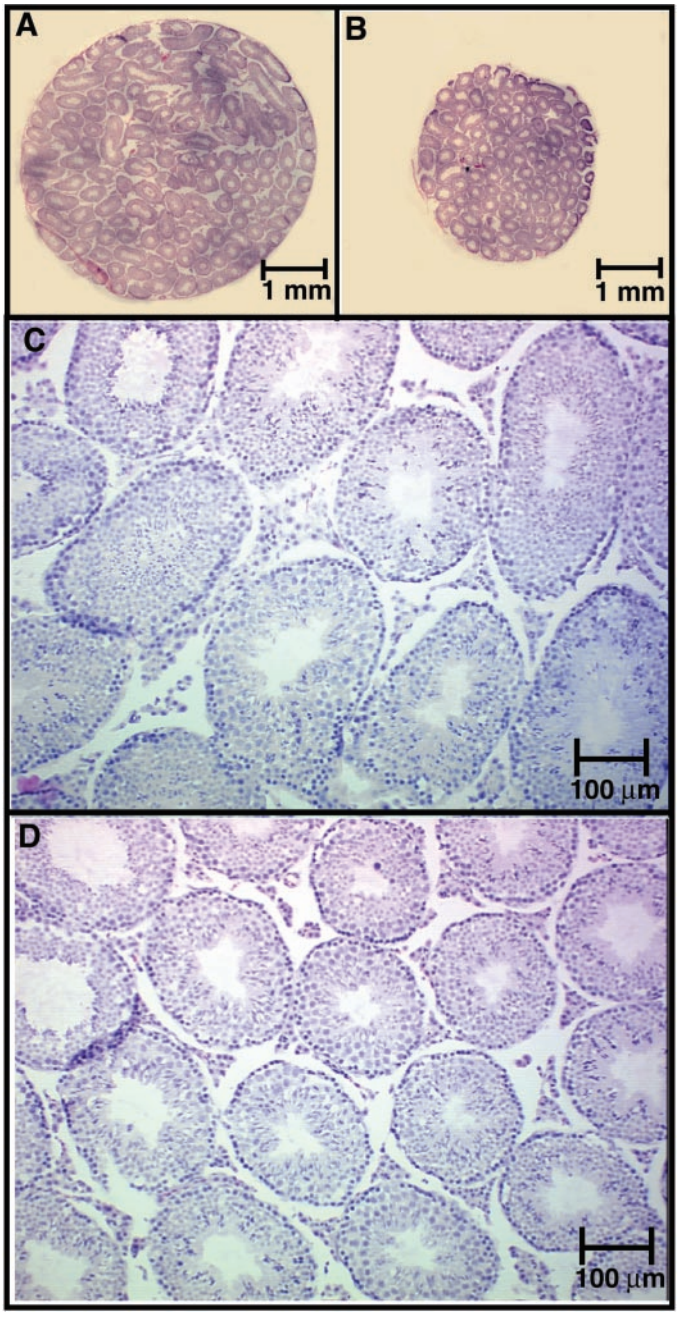

FIG. 4. Testicular histology of MT-α male mice and wild-type mice. Testes were prepared as described in Fig. 4 and cut into 4- to 6-μm sections. A, Cross-section of a wild-type testis; B, cross-section of a testis from an MT-α transgenic littermate; C, cross-sections of seminiferous tubules from a wild-type testis; D, cross-sections of seminiferous tubules from an MT-α transgenic testis. Magnification, $\times$11 in A and B and $\times$100 in C and D.

Steroid hormone profiles

To establish the effects of transgene expression on ovarian steroidogenesis, RIA was performed to determine serum levels of T and E for MT-α female mice. T levels were increased in MT-α transgenic female mice from both lines compared with wild-type female mice (Fig. 5A). Conversely, E levels were slightly lower in MT-α line C transgenic female mice (Fig. 5B), and uterine weights were also reduced (wild-

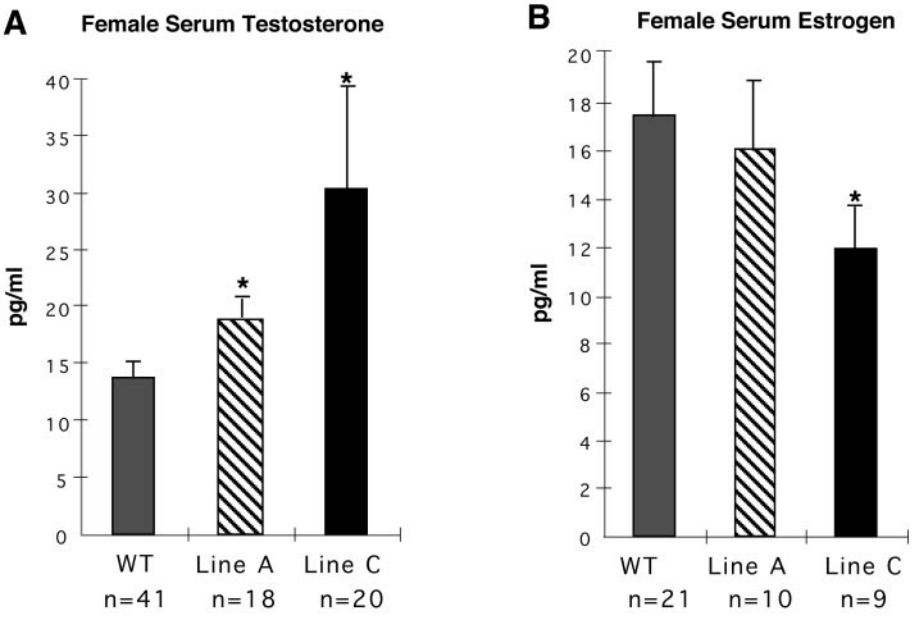

FIG. 5. Serum steroid hormone levels for female MT-α and wild-type mice. A, T levels for female wild-type and MT-α transgenic mice; B, E levels for female wild-type and MT-α transgenic mice. WT, Wild-type control mice (CD-1; Charles River Laboratories, Inc., Wilmington, MA). Shown are mean values ± SEM. Statistical analysis was performed using a *t* test. Both line A and line C T levels are significantly different from those of wild-type mice, whereas line C E levels are significantly different from those of wild-type mice ($P < 0.05$).

type, 152.9 ± 36.0 mg, n = 6; line A, 98.0 ± 10.0 mg, n = 5; line C, 105.0 ± 4.4 mg, n = 5).

GnRH antagonist treatment

The abnormal gonadotropin ratio in MT-α mice is in part responsible for reduced fertility, as discussed in the accompanying paper. To determine if the gonadotropin environment also contributed to the observed ovarian pathogenesis, FSH and LH levels were suppressed by chronically blocking GnRH action with the GnRH antagonist Cetrorelix (Asta Medica). If the perturbations in the gonadotropins induced the observed ovarian cysts, then suppressing these hormones should prevent the formation of ovarian cysts.

Six-week-old female mice were treated biweekly (every 84 h) with the GnRH antagonist Cetrorelix until the animals reached 6 months of age. Normally, most MT-α female mice exhibit ovarian cysts by 6 months of age, as previously discussed (Table 1). Serum hormone levels of FSH and LH were measured and found to be significantly repressed, indicating that the antagonist treatment was effective (Fig. 6). For vehicle-treated mice, LH levels were variable and were not observed to be significantly greater in MT-α females compared with wild type. The disparity between these (vehicle-treated) LH levels and the increased LH measurements reported in the accompanying paper is likely attributable to the fact that the animals used in the antagonist study were not matched for estrous cycle stage. FSH levels were greatly suppressed in vehicle-treated transgenic mice *vs.* vehicle-treated wild-type mice, consistent with our previous findings. Examination of ovarian morphology from antagonist-treated control mice showed a reduction in ovarian size and the absence of corpora lutea, again indicating that the GnRH antagonist was effective (Fig. 7, A and B). In Cetrorelix-treated transgenic mice, ovarian cysts persisted (Fig. 7, C and D). However, the morphology of the ovarian cysts in the antagonist-treated animals was quite different from that seen in vehicle-treated transgenic females (Fig. 7, C and D). Ovaries from antagonist-treated mice often exhibited extended and fluid-filled bursal sacs, but the internal ovarian cysts were generally smaller that those observed in vehicle-treated transgenic mice. The overall percentage of MT-α transgenic female mice that developed ovarian cysts was reduced by 15–20% compared with vehicle-treated MT-α transgenic female mice (Fig. 8). Thus, although the cyst phenotype is somewhat attenuated by chronic gonadotropin inhibition, ovarian cysts persist, consistent with a potential direct effect of the inhibin α-subunit transgene on the ovary.

Discussion

Gametogenesis and steroidogenesis are the two primary functions of the gonad. We have shown in the accompanying paper that the expression of an inhibin α-transgene has a negative impact on gamete production and fertility in MT-α transgenic mice. In the present study, we focus on changes in ovarian steroidogenesis and on several intriguing ovarian pathologies, including expansion of the bursal sac, development of polyovular follicles, and formation of cystic follicles, all of which suggest a disruption of normal folliculogenesis. Although these pathologies might be explained by the altered gonadotropin ratios in MT-α transgenic mice, our findings using chronic GnRH antagonism to suppress FSH and LH are consistent with a direct effect of the inhibin α-subunit transgene on ovarian steroidogenesis; additionally, they are in agreement with observed paracrine effects of inhibin on thecal cell androgen production in cell culture systems (28).

MT-α female transgenic mice have several ovarian phenotypes similar to transgenic mice overexpressing the LH β-subunit and ER-deficient mice, which also exhibit ovarian cysts (29–33). In addition to the commonality of cystic ovaries, all of the discussed genetic mouse models display aberrant hormone levels, specifically increased LH and T. The LHβ transgenic mice have increased LH, increased androgens, and, in the specific CF-1 genetic background, the females develop ovarian tumors. Both LH and T are increased

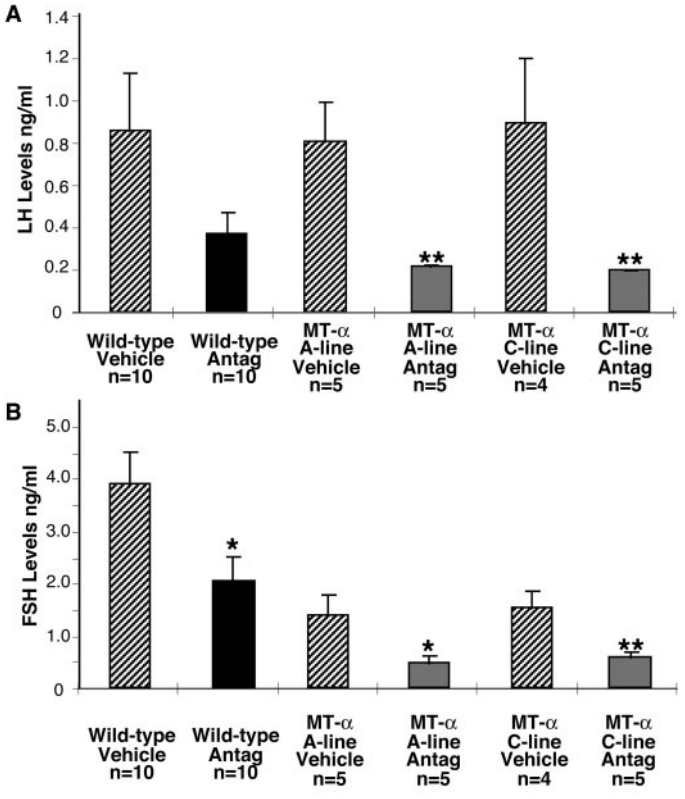

FIG. 6. MT-α and wild-type female mice (CD-1 genetic strain; Charles River Laboratories, Inc.) were treated with the GnRH antagonist Cetrorelix (Asta Medica; 10 mg/kg body weight) every 84 h for 4.5 months. At 6 months of age, serum gonadotropin measurements were performed. Serum hormone levels of LH and FSH are shown for both GnRH antagonist-treated (Cetrorelix) and vehicle-treated (water) mice. All statistical analyses were performed using two-way ANOVA with variance indicated by SEM, and statistical significance is represented by P values. A, LH levels of antagonist-treated mice *vs.* vehicle-treated mice (**, $P < 0.01$); B, FSH levels of antagonist-treated mice *vs.* vehicle-treated mice (*, $P < 0.05$). The number of females treated in each group is shown (n).

as early as 2 wk of age, resulting in the later development of gonadotropin-dependent hyperandrogenemia, precocious puberty, and hemorrhagic ovarian cysts (29, 30). E receptor-deficient mice (ERKO) also exhibit hemorrhagic ovarian cysts and a 10-fold increase in serum E2 and T (31–33). The cyst formation in ERKO mice may be attributable to increased LH resulting from the block in the E negative feedback loop. Although MT-α female mice exhibit ovarian cysts and increased T and LH, the pathology of MT-α cysts differs considerably from those observed in the LHβ or ERKO mice. The cysts from MT-α female mice are not hemorrhagic, except in a few rare cases, and are often associated with a distended bursal sac filled with fluid, unlike the hemorrhagic cysts observed in these other models.

The hormone profile of MT-α female mice resembles that of human polycystic ovarian syndrome (PCOS), which is characterized by increased androgen levels, increased LH levels, and anovulation (34, 35). In some studies, increased serum levels of inhibin A and inhibin B and increased follicular fluid inhibin levels have been associated with PCOS (13–15). Conversely, other studies have reported no link between high inhibin levels and PCOS (36, 37). The mechanisms underlying PCOS are not known, but evidence indicates that alterations in the endocrine, paracrine, and autocrine control of folliculogenesis are involved. PCOS is likely to be one example of a group of larger disorders that result in functional ovarian hyperandrogenism, for which the primary abnormality is gonadotropin-dependent hyperandrogenemia (38). Recent cell culture studies with thecal cells isolated from PCOS ovaries suggest that there is an increase in the steroidogenic activity of these cells, including changes in the androgen biosynthetic pathway (39). Despite some of the similarities in hormonal profile, the ovarian cysts from MT-α females are very different morphologically from the cysts observed in women with PCOS. The transgenic mouse cysts are massive and are usually limited to one to three cysts per ovary; they would appear to represent developed follicles that fail to appropriately ovulate. The cysts from PCOS ovaries are much smaller, subcapsular, and more numerous, representing a state of arrested early follicular maturation (38). Thus, the altered gonadotropin and steroid levels result in very distinct ovarian pathologies in this mouse model and in the human disease.

A related ovarian pathology, ovarian hyperstimulation syndrome, is characterized by massive ovarian enlargement and ovarian cysts after exogenous administration of human CG (hCG) (40). The ovarian cysts from women with ovarian hyperstimulation syndrome in many respects resemble MT-α transgenic ovarian cysts. Although the pathophysiology of the syndrome is still unclear, it is reported that treatment with hCG or LH causes increased permeability of ovarian capillary vessels, resulting in follicular cysts (40). Currently, several proteins such as vascular endothelial factor and factors of the renin-angiotensin system are believed to be responsible for stimulating increased vascular permeability after ovulation induction. In severe cases, vascular leakage can lead to fluid accumulation, ascites, and greatly enlarged ovaries with follicular and luteal cysts (41). The twice-daily treatment of rats with subovulatory doses of hCG results in the development of large ovarian cysts, suggesting that long-term exposure to LH is a factor in ovarian cyst formation (42). Cyst formation in MT-α transgenic mice may be associated with increased ovarian vessel permeability, although this has not been directly investigated. Consistent with a perturbation in vascular permeability is the pronounced distention of the bursal sac and the accumulation of fluid that is observed in most MT-α transgenic ovaries.

FSH and LH are important modulators of ovarian steroidogenesis and folliculogenesis, and the abnormal gonadotropin environment in MT-α transgenic females appears to contribute to the reduced fertility of these mice, as described in the accompanying paper. It is also likely that the reduction in serum FSH levels in the MT-α transgenic mice contributes to the ovarian and testicular growth phenotypes. Morphological examination of MT-α ovaries revealed a decrease in ovarian size and fewer corpora lutea and antral follicles compared with wild-type littermates. The MT-α ovarian morphology is similar in some respects to that of the activin receptor type II-deficient mouse and the follistatin overexpression transgenic mouse. Activin opposes inhibin function by stimulating the secretion of FSH from the anterior pitu-

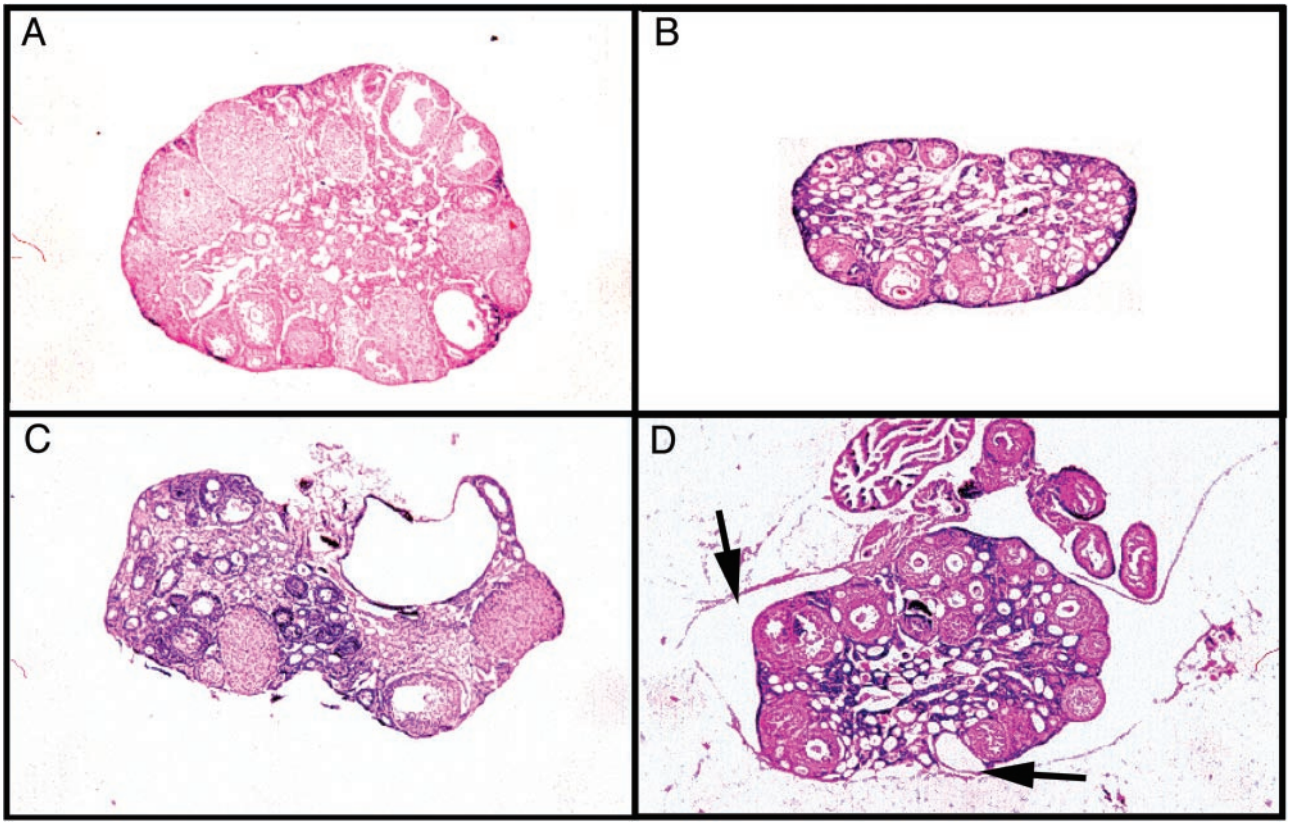

FIG. 7. MT-α and wild-type females were treated with the GnRH antagonist Cetrorelix (10 mg/kg body weight) every 84 h for 4.5 months. At 6 months of age, ovarian morphology was examined. The ovarian morphology of antagonist-treated and vehicle-treated MT-α and wild-type mice is shown. A, Vehicle-treated wild-type ovary; B, Cetrorelix-treated wild-type ovary; C, vehicle-treated MT-α transgenic ovary; D, Cetrorelix-treated MT-α transgenic ovary. Note the absence of corpora lutea and the reduction in ovarian size in antagonist-treated female mice. The antagonist-treated MT-α ovary still exhibits internal ovarian cysts, although smaller in size (*arrow at bottom*), and an extended bursal sac (*arrow at top*).

itary. Activin receptor type II-deficient mice are defective for activin signaling and exhibit suppressed FSH levels, small ovaries, and fewer corpora lutea (43). Follistatin is an activin-binding protein that is able to act *in vivo* as an activin antagonist (44). Some lines of follistatin overexpression transgenic mice are infertile, with small ovaries containing follicles blocked at various stages of follicular development, and these mice also have reduced FSH levels (45). MT-α transgenic male mice exhibit a reduction in testis size, tubule volume, and sperm numbers. MT-α transgenic males, unlike MT-α females, are fertile. MT-α transgenic males exhibit a strikingly similar phenotype to both FSH-deficient male mice and FSH receptor-deficient males (46, 47). The common phenotype is the reduction in testis volume and sperm numbers. Despite abnormal FSH levels and sperm production, MT-α transgenic males are fully fertile, thus supporting the hypothesis that FSH is not essential for male fertility in the rodent (46, 47).

Altered gonadotropin levels might also be expected to be causative in the ovarian pathologies and cyst formation observed in these mice. Administration of excess LH or hCG to pregnant or hypothyroid rats is known to cause the formation of ovarian follicular cysts (42, 48). However, in our studies, chronic suppression of both LH and FSH release in MT-α female mice using the GnRH antagonist Cetrorelix failed to block cyst formation. Ovarian cysts from the antagonist-treated MT-α females are smaller in size, but they occur at about the same frequency as in control animals. In addition, fluid accumulation in the ovarian bursal sac continue to occur in antagonist-treated animals. This suggests a gonadotropin-independent action of the inhibin α-subunit transgene product, most likely at the level of the ovary. An attractive possibility is that excess ovarian inhibin results in increased ovarian androgen production. Inhibin is reported to stimulate LH-induced androgen production by rat thecal or Leydig cells in cultures (11, 28), and T levels are increased in transgenic mice. Consistent with this idea, T or dehydroepiandrosterone treatment of rats also results in the formation of ovarian cysts, indicating that steroids alone can induce ovarian pathologies similar to those observed in the MT-α transgenic mice (49, 50). Alterations in ovarian steroidogenesis, therefore, may be the mechanism by which the inhibin transgene induces these complex ovarian pathologies. As discussed in the accompanying paper, this action may represent a combination of increased inhibin levels and suppressed activin levels, resulting in an altered inhibin-to-activin ratio. These studies support an important role for inhibin and activin in the maintenance of normal ovarian follicular development and ovulation.

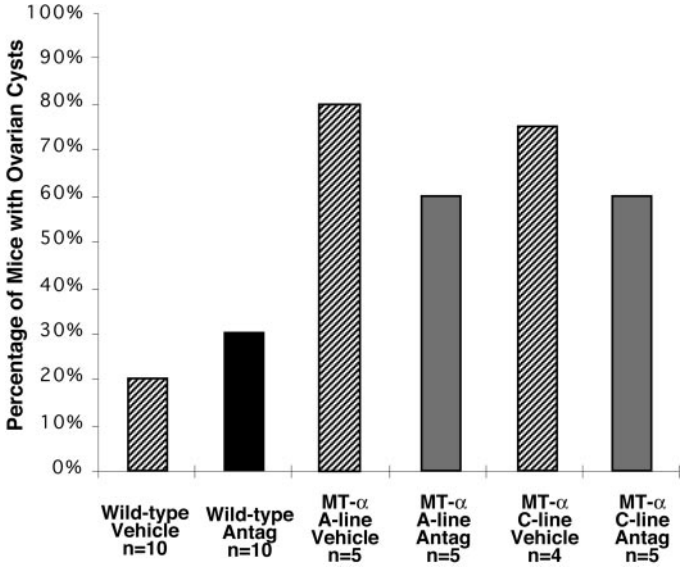

FIG. 8. Percentage of mice that exhibited ovarian cysts after a 4.5-month treatment with the GnRH antagonist Cetrorelix or vehicle (water). The number of female mice treated in each group is shown (n). There was no significant difference in the rate of cyst development between antagonist-treated mice and placebo-treated mice for each group (MT-α line A transgenic mice, MT-α line C transgenic mice, or wild-type mice). There was a significant difference in the rate of cyst development between placebo-treated wild-type and placebo-treated transgenic mice. Statistical analyses were performed using χ^2 goodness of fit based on 1 degree of freedom and χ^2 sums greater than a 0.95 P level.

Acknowledgments

We thank Brigitte Mann for performing the steroid RIAs and Dr. Jon Levine, director of the P30 RIA Core. We thank Dr. Wylie Vale for donating the inhibin α-subunit RIA reagents and Asta Medica for donating the GnRH antagonist Cetrorelix. We also thank Dr. Teresa Woodruff for her comments on the manuscript.

Received May 22, 2001. Accepted July 11, 2001.

Address all correspondence and requests for reprints to: Kelly E. Mayo, Ph.D., Department of Biochemistry, Molecular Biology, and Cell Biology, Northwestern University, Evanston, Illinois 60208. E-mail: k-mayo@northwestern.edu.

This work was supported by NIH Program Project Grant HD-21921 and NIH Center Grant P30-HD-28048 (to K.E.M.). M.L.M. was supported in part by NIH Training Grants HD-07068 and GM-08449. B.-N.C. was supported in part by the Lalor Foundation.

* Present address: Division of Life Science, The Catholic University of Korea, Puchon, South Korea 421-743.

References

1. **Ling N, Ying SY, Ueno N, Esch F, Denoroy L, Guillemin R** 1985 Isolation and partial characterization of a Mr 32,000 protein with inhibin activity from porcine follicular fluid. Proc Natl Acad Sci USA 82:7217–7221
2. **Robertson DM, Foulds LM, Leversha L, Morgan FJ, Hearn MT, Burger HG, Wettenhall RE, de Krester DM** 1985 Isolation of inhibin from bovine follicular fluid. Biochem Biophys Res Commun 126:220–226
3. **Miyamoto K, Hasegawa Y, Fukuda M, Nomura M, Igarashi M, Kangawa K, Matsuo H** 1985 Isolation of porcine follicular fluid inhibin of 32K daltons. Biochem Biophys Res Commun 129:396–403
4. **Rivier J, Spiess J, McClintock R, Vaughan J, Vale W** 1985 Purification and partial characterization of inhibin from porcine follicular fluid. Biochem Biophys Res Commun 133:120–127
5. **Vale W, Rivier J, Vaughan J, McClintock R, Corrigan A, Woo W, Karr D, Spiess J** 1986 Purification and characterization of an FSH releasing protein from porcine ovarian follicular fluid. Nature 321:776–779
6. **Ling N, Ying SY, Ueno N, Shimasaki S, Esch F, Hotta M, Guillemin R** 1986 Pituitary FSH is released by a heterodimer of the β subunits from the two forms of inhibin. Nature 321:779–782
7. **Woodruff TK, Lyon RJ, Hansen SE, Rice GC, Mather JP** 1990 Inhibin and activin locally regulate rat ovarian folliculogenesis. Endocrinology 127:3196–3205
8. **Mather JP, Attie KM, Woodruff TK, Rice GC, Phillips DM** 1990 Activin stimulates spermatogonial proliferation in germ-Sertoli cell cocultures from immature rat testis. Endocrinology 127:3206–3214
9. **LaPolt PS, Hsueh AJW** 1991 Molecular basis of inhibin production. Mol Cell Endocrinol 2:449–463
10. **LaPolt PS, Soto D, Su JG, Campen CA, Vaughan J, Vale W, Hsueh AJ** 1989 Activin stimulation of inhibin secretion and messenger RNA levels in cultured granulosa cells. Mol Endocrinol 3:1666–1673
11. **Hsueh AJ, Dahl KD, Vaughan J, Tucker E, Rivier J, Bardin CW, Vale W** 1987 Heterodimers and homodimers of inhibin subunits have different paracrine action in the modulation of luteinizing hormone-stimulated androgen biosynthesis. Proc Natl Acad Sci USA 84:5082–5086
12. **Tsafriri A, Vale W, Hsueh AJ** 1989 Effects of transforming growth factors and inhibin-related proteins on rat preovulatory graafian follicles in vitro. Endocrinology 125:1857–1862
13. **Barnes RB** 1998 The pathogenesis of polycystic ovary syndrome: lessons from ovarian stimulation studies. J Endocrinol Invest 21:567–579
14. **Anderson RA, Groome NP, Baird DT** 1998 Inhibin A and inhibin B in women with polycystic ovarian syndrome during treatment with FSH to induce monoovulation. Clin Endocrinol 48:577–584
15. **Tanabe K, Saiji A, Park JY, Kohriyama S, Sano Y, Nakamura Y, Iizuka R** 1990 The role of inhibin in women with polycystic ovary syndrome (PCOS). Horm Res(Suppl 2)33:10–17
16. **Lappohn RE, Burger HG, Bouma J, Bangah M, Krans M, De Bruijn HWA** 1989 Inhibin as a marker for granulosa cell tumors. N Engl J Med 321:790–793
17. **Nishida M, Jimi S, Haji M, Hayashi I, Kai T, Tasaka H** 1991 Juvenile granulosa cell tumor in association with a high serum inhibin level. Gynecol Oncol 40:90–94
18. **Frias Jr AE, Li H, Keeney GL, Podratz KC, Woodruff TK** 1999 Preoperative serum level of inhibin A is an independent prognostic factor for the survival of postmenopausal women with epithelial ovarian carcinoma. Cancer 85: 465–471
19. **Piquette GN, Kenney RM, Sertich PL, Yamoto M, Hsueh AJ** 1990 Equine granulosa-theca cell tumors express inhibin α- and β_A-subunit messenger ribonucleic acids and proteins. Biol Reprod 43:1050–1057
20. **Matzuk MM, Finegold MJ, Su JG, Hsueh AJ, Bradley A** 1992 α-Inhibin is a tumour-suppressor gene with gonadal specificity in mice. Nature 360:313–319
21. **Matzuk MM, Finegold MJ, Mather JP, Krummen L, Lu H, Bradley A** 1994 Development of cancer cachexia-like syndrome and adrenal tumors in inhibin-deficient mice. Proc Natl Acad Sci USA 91:8817–8821
22. **Glanville N, Durnam DM, Palmiter RD** 1981 Structure of mouse metallothionein-I gene and its mRNA. Nature 292:267–269
23. **Palmiter RD, Norstedt G, Gelinas RE, Hammer RE, Brinster RL** 1983 Metallothionein-human GH fusion genes stimulate growth of mice. Science 222: 809–814
24. **Ackland JF, D'Agostino J, Ringstrom SJ, Hostetler JP, Mann BG, Schwartz NB** 1990 Circulating radioimmunoassayable inhibin during periods of transient follicle-stimulating hormone rise: secondary surge and unilateral ovariectomy. Biol Reprod 43:347–352
25. **Vaughan JM, Rivier J, Corrigan AZ, McClintock R, Campen CA, Jolley D, Vogelmayr JK, Bardin CW, Rivier C, Vale W** 1989 Detection and purification of inhibin using antiserum generated against synthetic peptide fragments. Methods Enzymol 168:588–617

25a. **Cho B-N, McMullen M, Peil L, Yates CJ, Mayo K** 2001 Reproductive deficiencies in transgenic mice expressing the rat inhibin α-subunit gene. Endocrinology 142:4994–5004

26. **Thung PJ, Boot LM, Muhlbock O** 1956 Senile changes in the oestrous cycle and in ovarian structure in some inbred strains of mice. Acta Endocrinol 23:8–32
27. **Albertini DF, Carabatsos MJ** 1998 Comparative aspects of meiotic cell cycle control in mammals. J Mol Med 76:795–799
28. **Hillier SG, Yong EL, Illingworth PJ, Baird DT, Schwall RH, Mason AJ** 1991 Effect of recombinant inhibin on androgen synthesis in cultured human thecal cells. Mol Cell Endocrinol 75:R1–R6
29. **Risma KA, Clay CM, Nett TM, Wagner T, Yun J, Nilson JH** 1995 Targeted overexpression of luteinizing hormone in transgenic mice leads to infertility, polycystic ovaries, and ovarian tumors. Proc Natl Acad Sci USA 92:1322–1326
30. **Risma KA, Hirshfield AN, Nilson JH** 1997 Elevated luteinizing hormone in prepubertal transgenic mice causes hyperandrogenemia, precocious puberty, and substantial ovarian pathology. Endocrinology 138:3540–3547
31. **Couse JF, Curtis SW, Washburn TF, Lindzey J, Golding TS, Lubahn DB, Smithies O, Korach KS** 1995 Analysis of transcription and estrogen insensitivity in the female mouse after targeted disruption of the estrogen receptor gene. Mol Endocrinol 9:1441–1454
32. **Lindzey J, Korach KS** 1997 Developmental and physiological effects of estrogen receptor gene disruption in mice. Trends Endocrinol Metab 8:137–145
33. **Schomberg DW, Couse JF, Mukherjee A, Lubahn DB, Sar M, Mayo KE,**

Korach KS 1999 Targeted disruption of the estrogen receptor-α gene in female mice: characterization of ovarian responses and phenotype in the adult. Endocrinology 140:2733–2744
34. **Franks S** 1991 The ubiquitous polycystic ovary. J Endocrinol 129:317–319
35. **Barbieri RL** 1991 Polycystic ovarian disease. Annu Rev Med 42:199–204
36. **Buckler HM, McLachlan RI, MacLachlan VB, Healy DL, Burger HG** 1988 Serum inhibin levels in polycystic ovary syndrome: basal levels and response to luteinizing hormone-releasing hormone agonist and exogenous gonadotropin administration. J Clin Endocrinol Metab 66:798–803
37. **Lambert-Messerlian G, Taylor A, Leykin L, Isaacson K, Toth T, Chang Y, Schneyer A** 1997 Characterization of intrafollicular steroid hormones, inhibin, and follistatin in women with and without polycystic ovarian syndrome following gonadotropin stimulation. Biol Reprod 57:1211–1216
38. **Ehrmann DA, Barnes RB, Rosenfield RL** 1995 Polycystic ovary syndrome as a form of functional ovarian hyperandrogenism due to dysregulation of androgen secretion. Endocr Rev 16:322–353
39. **Nelson VL, Legro RS, Strauss III JF, McAllister JM** 1999 Augmented androgen production is a stable steroidogenic phenotype of propagated theca cells from polycystic ovaries. Mol Endocrinol 13:946–957
40. **Elchalal U, Schenker JG** 1997 The pathophysiology of ovarian hyperstimulation syndrome: views and ideas. Hum Reprod 12:1129–1137
41. **Dourron NE, Williams DB** 1996 Prevention and treatment of ovarian hyperstimulation syndrome. Semin Reprod Endocrinol 14:355–365
42. **Bogovich K** 1991 Induction of ovarian follicular cysts in the pregnant rat by human chorionic gonadotropin. Biol Reprod 45:34–42
43. **Matzuk MM, Kumar TR, Bradley A** 1995 Different phenotypes for mice deficient in either activins or activin receptor type II. Nature 374:356–360
44. **Nakamura T, Takio K, Eto Y, Shibai H, Titani K, Sugino H** 1990 Activin-binding protein from rat ovary is follistatin. Science 247:836–838
45. **Guo Q, Kumar TR, Woodruff T, Hadsell LA, DeMayo FJ, Matzuk MM** 1998 Overexpression of mouse follistatin causes reproductive defects in transgenic mice. Mol Endocrinol 12:96–106
46. **Kumar TR, Wang Y, Lu N, Matzuk MM** 1997 Follicle stimulating hormone is required for ovarian follicle maturation but not male fertility. Nat Genet 15:201–204
47. **Dierich A, Sairam MS, Monaco L, Fimia GM, Gansmuller A, LeMeur M, Sassone-Corsi P** 1998 Impairing follicle-stimulating hormone (FSH) signaling in vivo: targeted disruption of the FSH receptor leads to aberrant gametogenesis and hormonal imbalance. Proc Natl Acad Sci USA 95:13612–13617
48. **Lee MT, Brout BC, Adams WC** 1986 Hormonal changes during the early development of ovarian cysts in the rat. Biol Reprod 35:542–548
49. **Roy S, Mahesh VB, Greenblat RB** 1962 Effects of dehydroepiandrosterone and D4-androstenedione on the reproductive organs of female rats: production of cystic changes in the ovary. Nature 196:42–43
50. **Roy S, Datta JK** 1979 Counteraction of testosterone-induced suppression of the pituitary-ovarian axis in rats by flutamide. Horm Res 11:61–68